Evaluation of Building Damage and Tsunami Inundation Based on Satellite Images and GIS Data Following the 2010 Chile Earthquake

Yoshihisa Maruyama,[a)] M.EERI, Fumio Yamazaki,[a)] M.EERI, Shizuko Matsuzaki,[a)] Hiroyuki Miura,[b)] and Miguel Estrada[c)]

This paper presents the results of a field survey conducted by the authors after the 2010 Chile earthquake. The authors visited the affected area about a month after the earthquake. The usefulness of satellite images captured after the earthquake to detect damaged buildings in Concepción is discussed, compared with the field photos taken by the authors. GIS datasets for the damage levels of buildings in Talca and the tsunami-inundated areas in Talcahuano, Dichato, and Constitución are constructed in this study. The GIS dataset for the damage levels of buildings in Talca is compared with the satellite images, and the possibility of detecting damage to adobe houses is investigated. Further, a series of fundamental analyses are performed using a digital elevation model (DEM) that is constructed from ASTER images (ERSDAC 2009), and the usefulness of the DEM is evaluated comparing with the field survey results. [DOI: 10.1193/1.4000023]

INTRODUCTION

The 2010 Chile earthquake occurred off the coast of the Maule Region of Chile on 27 February 2010 at 03:34 local time (06:34 UTC), with a magnitude of 8.8 on the moment magnitude scale. The epicenter was offshore from the Maule Region, approximately 335 km southwest of Santiago, the capital of Chile, and 105 km north–northeast of Chile's second-largest city, Concepción. This earthquake fills a well-studied seismic gap between the source areas of the largest ever recorded 1960 Great Valdivia earthquake (M 9.5), and the 1985 Valparaiso earthquake (M 7.8; Ruegg et al. 2009). It is reported that a severe ground motion was felt widely in Chile, and the peak ground acceleration exceeded 900 cm/s^2 at Angol Station (Boroschek et al. 2010). In addition, extensive damage was also caused by the tsunami. The total economic loss estimates range from US$15 to $30 billion, which correspond to 10% to 15% of Chile's real GDP. According to a report on the scene, the actual death toll was 486 as of 8 March 2010, and approximately 370,000 homes were damaged (Bray and Frost 2010).

a) Graduate School of Engineering, Chiba University, 1-33 Yayoi-cho, Inage-ku, Chiba 263-8522, Japan
b) Interdisciplinary Graduate School of Science and Engineering, Tokyo Institute of Technology, 4259 Nagatsuta, Midori-ku, Yokohama, 226-8502, Japan
c) Japan Peru Center for Earthquake Engineering and Disaster Mitigation, National University of Engineering, Peru, Av. Túpac Amaru 1150, Lima 25, Perú

Earthquake Spectra, Volume 28, No. S1, pages S165–S178, June 2012; © 2012, Earthquake Engineering Research Institute

The authors visited the affected area about a month after the event, as part of an international research project titled "Enhancement of earthquake and tsunami disaster mitigation technology in Peru" (Yamazaki et al. 2010), which is under the research program Science and Technology Research Partnership for Sustainable Development (SATREPS) supported by the Japan Science and Technology Agency (JST) and the Japan International Cooperation Agency (JICA; JST 2008). The lessons learned from the 2010 Chile earthquake are expected to apply to the earthquake disaster mitigation technologies in Peru because the two countries have common regional tectonics and social surroundings.

In this paper, the results of the field survey performed by the team consisting of the present authors are presented. The usefulness of satellite images to detect damaged buildings in Constitución, compared to the field photos taken by the authors, is. The spatial damage data, topographical maps, and satellite images provided by different institutions are compiled by the geographical information system (GIS), and the preliminary analyses are conducted. Specifically, the GIS dataset to show the damage levels of buildings in Talca is employed to evaluate the applicability of satellite images to detect damage to adobe and unreinforced masonry buildings, which are the common construction types for both in Chile and Peru. In addition, a digital elevation model (DEM) constructed for all the land on the earth (ASTER GDEM) is also employed to reveal the characteristics of the tsunami-inundated areas. The accuracy of the topographical features obtained from the worldwide DEM is discussed comparing with the results from other field survey group.

COMPARISON BETWEEN SATELLITE IMAGES AND FIELD PHOTOS TO DETECT DAMAGED BUILDINGS IN CONCEPCIÓN

The authors arrived in Santiago on 2 April 2010. We drove to Concepción the next day and visited the tsunami-affected areas of Talcahuano, Dichato, and Constitución. We moved to Talca on 7 April and left Santiago on 8 April. Before leaving, we visited Valparaíso and Viña del Mar.

Concepción is the second-largest city in Chile, and its population is approximately 300,000. Concepción was affected by severe ground motion, with the MMI scale of VII (USGS 2010). Recent advancements in remote sensing technologies and their applications have made it possible to use remotely sensed imagery for estimating the damage distribution due to natural disasters (Rathje and Adams 2008). Among them, high-resolution optical satellite imagery, which has become available in the last decade, has made satellite remote sensing more useful in disaster management since even the damage status of individual buildings can be identified (Saito et al. 2004, Yamazaki et al. 2005, Eguchi et al. 2008).

As for the areas affected by the 2010 Chile earthquake, various kinds of satellite images were acquired and they were employed to detect the damage distribution after the event. WorldView-2, which was launched on 8 October 2009, observed Concepción on 6 March 2010 and fine images are available to detect damage to buildings. WorldView-2 provides the high-resolution, eight-band multispectral imagery. The spatial resolution of the panchromatic image is 0.5 m and that of the multispectral image is 2.0 m. By performing pan-sharpening, one can obtain a colored image with the resolution of 0.5 m.

Pan-sharpening is a technique that merges high-resolution panchromatic data with medium-resolution multispectral data to create a multispectral image with higher-resolution features (Campbell 2006).

Figure 1 shows the survey route in Concepción and the locations of photo shootings during our field survey. The six locations, identified as (a)–(f), were selected to compare the satellite images with the field photos taken by the authors in Figure 1. As for the pre-event satellite images, the images from Google Earth are used in Table 1. A reinforced concrete (RC) building with 21 stories was found at the site labeled (a), and its middle stories were seriously affected. It is reported that severe damage, including axial shortening of stories on the SW face and severe damage on the NW face, were found (EERI 2010a); however, this is not detected from the post-event satellite image. Because the image was captured with the large off-nadir angle (26.7°), the image was inclined only to make a shadow on the damaged face. An RC building, which fell down after the earthquake, was found at the site labeled (b) and it was obviously identified from the post-event image.

Unreinforced masonry buildings were severely damaged in the central city of Concepción, such as the site labeled (c). Although the spread of debris and the deformation of roofs are realized from the post-event image, the status of damage can not be observed so clearly. Cereal silos were affected by ground shaking at the site (d) and they are surely observed in the post-event satellite image. The Old Bío-Bío Bridge, constructed in the 1930s, collapsed because of the earthquake at the site (e) (EERI 2010b). The collapsed bridge girders are clearly seen from the post-event image. The Llacolen Bridge across the Bío-Bío River observed to have span collapse due to seismic lateral movement at the site (f). According to the field photo on the scene, a temporary steel truss bridge had been installed to allow traffic to cross the bridge. The construction of the temporary bridge girder is seen from the post-event satellite image.

CONSTRUCTION OF GIS FOR BUILDING DAMAGE IN TALCA

Talca is the capital of both Talca Province and the Maule Region. Its population is approximately 200,000, and it is approximately 250 km south of Santiago and 60 km northwest of the epicenter of the 2010 Chile Earthquake. According to the U.S. Geological Survey (USGS 2010), Talca was affected with a severe ground motion, VII on the MMI scale. About 8,000 people were in need of shelter because of the earthquake (EERI 2010c).

During our survey, we interviewed officials from Maule Regional Office to investigate the damage of buildings. As a result of our interview, an image file that shows the damage levels of buildings was provided. The polygons, which indicate the building lots, are classified into four levels, namely, to be removed, to be repaired, no damage, and under investigation. It should be noted that the image file was compiled with the damage dataset as of 31 March 2010.

In this study, the location of the image file was established in terms of map projections. The satellite image and road data presented in Google Earth were employed as a base map to georeference the image file. Then, the image file was converted to a GIS file

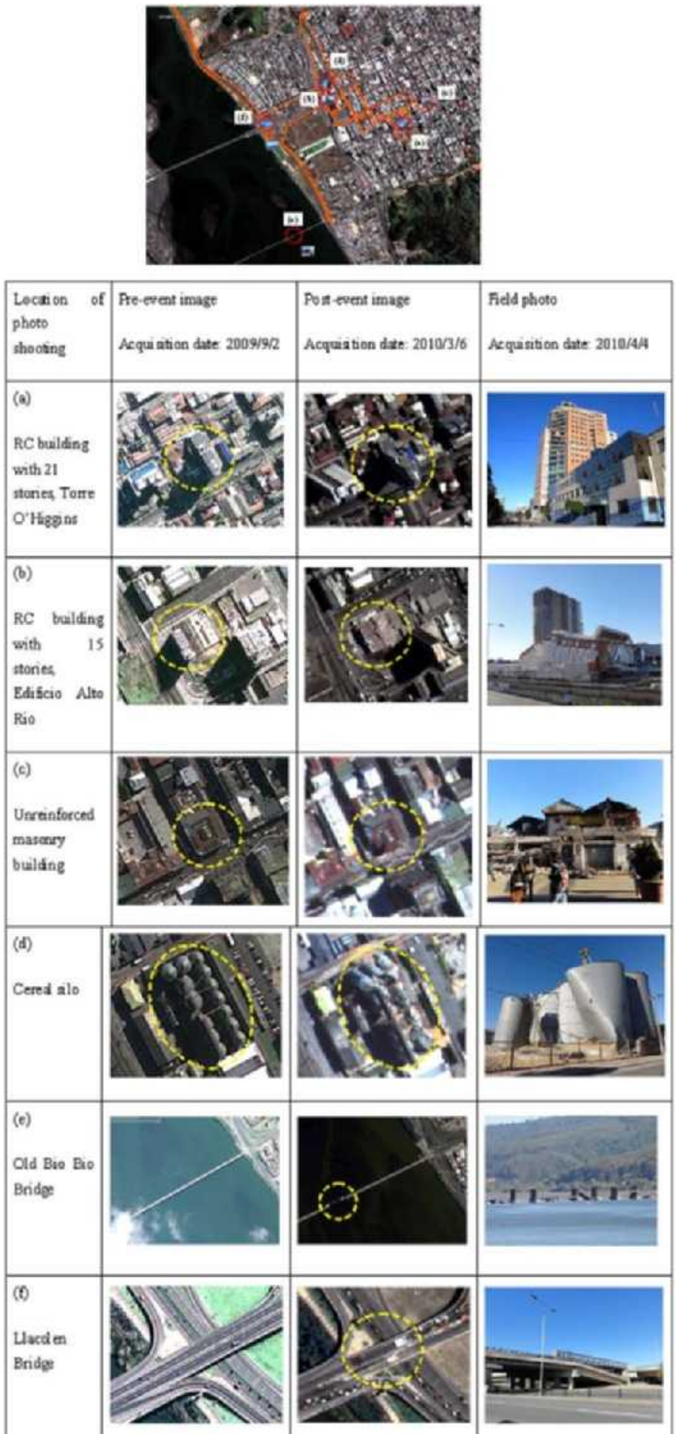

Figure 1. Survey route and the locations of photo shoots in Concepción and comparison between satellite images and field photos.

with polygons to identify the damage levels of buildings. Figure 2 shows the developed GIS file presented by Google Earth. We select the two areas in Figure 2 to show close-ups of the developed GIS file. This dataset consists of polygons only to show four levels of damage assessment. The information on building inventories related to seismic vulnerability is not available at this moment. Hence, it is difficult to consider the relationships among the damage ratio of buildings, the type of structure, and other structural properties in this paper.

In all, 5,617 polygons were projected to the map coordinate system. One thousand five hundred fifty-nine (27.8%), 1,872 (33.3%), and 1,864 (33.2%) buildings were classified as needing to be removed, to be repaired, and with no damage, respectively. The typical construction types in Talca are adobe and unreinforced masonry buildings, which are primarily used for older buildings with two to four stories (dating back to before the 1960s–70s). Modern buildings that were designed according to the current codes suffered minor, repairable damage, while a large number of adobe and unreinforced masonry buildings suffered significant damage (MCEER 2010).

Figure 3 shows the cumulative frequencies of the areas of building lots with respect to the damage level. The area of building lots can be estimated individually based on GIS functions because the image file was projected onto a map projection. The mean of all the

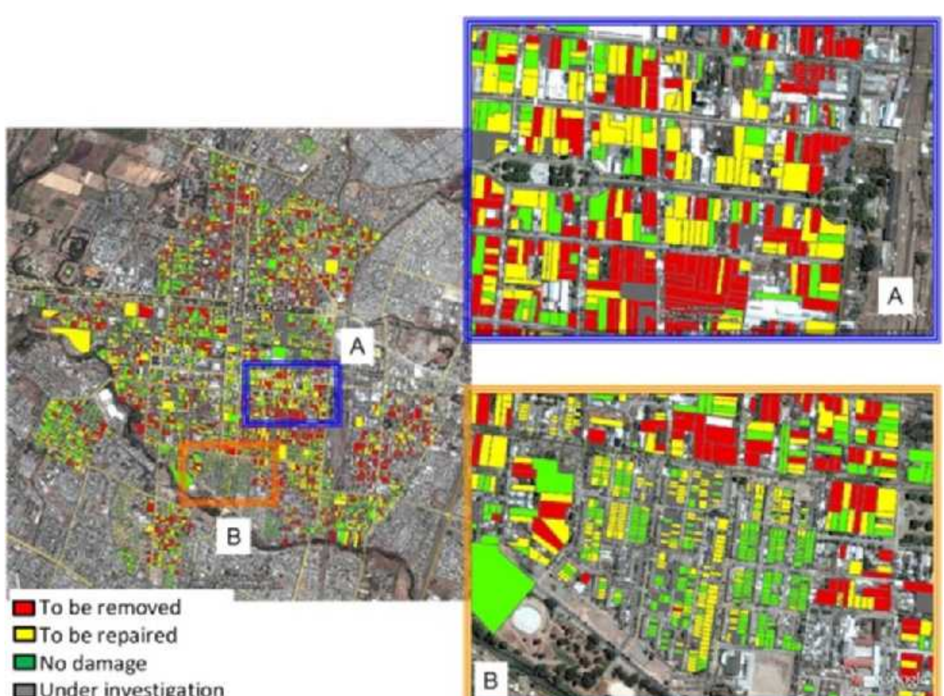

Figure 2. GIS file to show the damage levels of buildings in Talca.

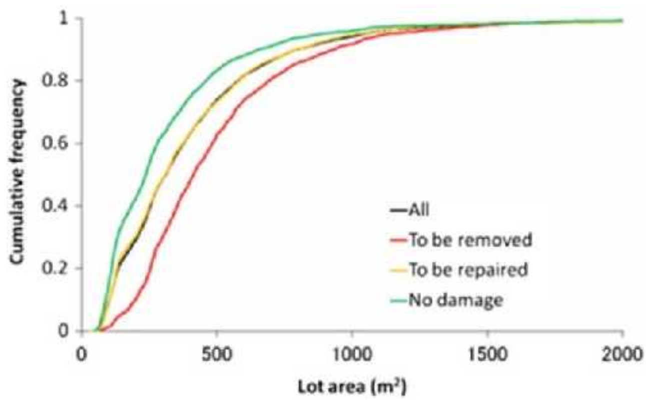

Figure 3. Cumulative frequencies of the areas of building lots with respect to the damage level. The red rectangles indicate the affected areas that were detected visually.

georeferenced areas was approximately 430 m^2 and was almost equal to that of the areas associated with the buildings to be repaired. The mean of the lot areas of the nondamaged buildings was approximately 340 m^2, which was considerably smaller than that of the buildings to be removed. On the basis of the results, it has been speculated that the newer buildings are constructed in relatively small lots (see the area indicated as zone B in Figure 2); however, the construction periods are not available at this moment. Additionally, adobe and unreinforced masonry buildings constructed in wider lots might be fragile to ground motion because of the lack of shear resistance. A more detailed investigation can be performed if the building inventories are available.

Using the post-event satellite image, the damaged buildings in Talca were visually inspected. The satellite image was observed by WorldView-2 on 10 March 2010, and the image presented on Google Earth with the acquisition date of 1 January 2008 was also employed as the pre-event image. The GIS file constructed in this study was employed as the benchmark data to evaluate the applicability of the high-resolution satellite images to grasp the damage distribution of adobe and unreinforced masonry buildings just after the earthquake.

Figure 4 shows the comparisons among the pre- and post-event satellite images and the GIS data to show the damage levels of buildings. A series of comparisons of the pre- and post-event images revealed that some of the affected buildings could be visually detected, but not all the damaged ones could be identified appropriately. Since the post-event image was captured with the large off-nadir angle (40.3°), the quality of image is not sufficient for visual damage inspection for adobe and reinforced masonry buildings. Moreover, the number of affected buildings whose roofs had completely collapsed is small in Talca. Hence, it can be concluded that the damaged buildings in Talca are difficult to detect through visual damage inspection using high-resolution optical satellite images.

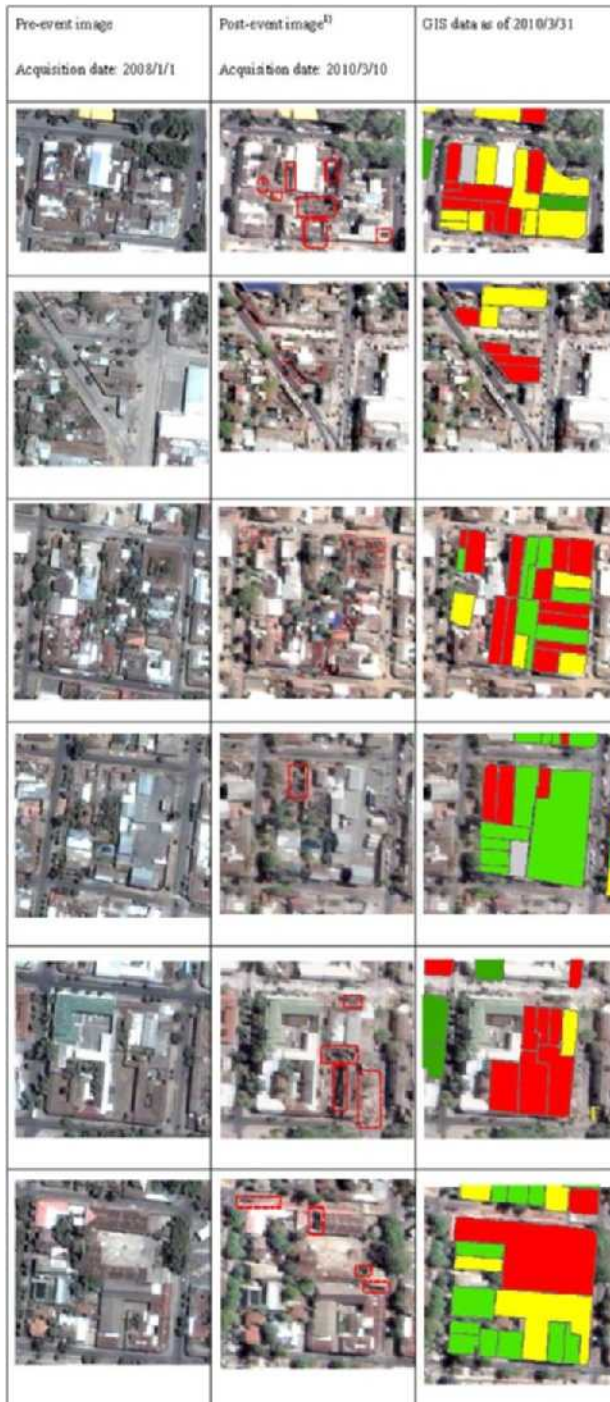

Figure 4. Comparison between satellite images and GIS data to show the damage levels of buildings in Talca.

DEVELOPMENT OF GIS FOR TSUNAMI-INUNDATED AREAS AND INVESTIGATION OF TOPOGRAPHICAL FEATURES BASED ON THE DIGITAL ELEVATION MODEL

The authors also visited the tsunami-inundated areas, for example, Talcahuano, Dichato, and Constitución. Constitución is located at the river mouth of the Maule River, and its population is approximately 40,000. Constitución was severely affected by tsunami, and the authors visited there on 6 April 2010. The Advanced Land Observing Satellite (ALOS), which was developed in the Japanese Earth observing satellite program and was launched on 24 January 2006, acquired the fine post-event image by AVNIR-2 for Constitución. Figure 8 compares the pre- and post-event false-color images. The pre-event image was captured on 2 December 2009. Vegetation in a false-color image appears to be red, and the healthier the vegetation, the brighter color red in the image (Campbell 2006). According to the close-ups, less vegetated areas are found in the islands in the Maule River and the areas along the river.

Various institutions released the maps to show the damage distribution at their Web sites after the 2010 Chile earthquake (ReliefWeb 2010). The tsunami-inundated areas interpreted from satellite and aerial images were published by National Office of Emergency of the Interior Ministry (ONEMI) of Chile (SNIT 2010). On the basis of the maps, the number of affected buildings and that of causalities were estimated. In this study, the tsunami-inundated area maps developed by ONEMI were projected onto a GIS system, and the topographical features were evaluated in terms of the elevation. The inundated areas in Talcahuano, Dichato, and Constitución were converted to the GIS data and compared with the digital elevation model (DEM). After the 2004 Indian Ocean tsunami, the tsunami-inundated areas were evaluated based on the Shuttle Radar Topography Mission (SRTM) dataset (Chen et al. 2005, Miura et al. 2006, Kouchi and Yamazaki 2007). The SRTM DEM with the

Figure 5. Comparison between pre- and post-event ALOS/AVNIR-2 satellite images that captured Constitución.

resolution of 30 m can be provided for the United States and that with the resolution of 90 m is available for the entire world (Jet Propulsion Laboratory 2009). The DEM employed in this study is the ASTER Global Digital Elevation Model (GDEM) developed by the Ministry of Economy, Trade, and Industry (METI) of Japan and the United States's National Aeronautics and Space Administration (NASA; ERSDAC 2009). The ASTER GDEM is a highly accurate DEM covering all the land on the earth with the spatial resolution of 30 m, and its standard deviation is 7 m to 14 m.

Figures 6–8 show the tsunami-inundated areas in Talcahuano, Dichato, and Constitución and the distributions of the elevation derived from the ASTER GDEM. The elevations in the inundated areas are lower than 20 m on the whole except for a certain area in Constitución. As shown in the figure, we set the two traverse lines in each inundated area. The elevations were extracted along the two lines. The extracted elevations are also illustrated in terms of the distance from the coastline. As for Line 2 in Constitución, the

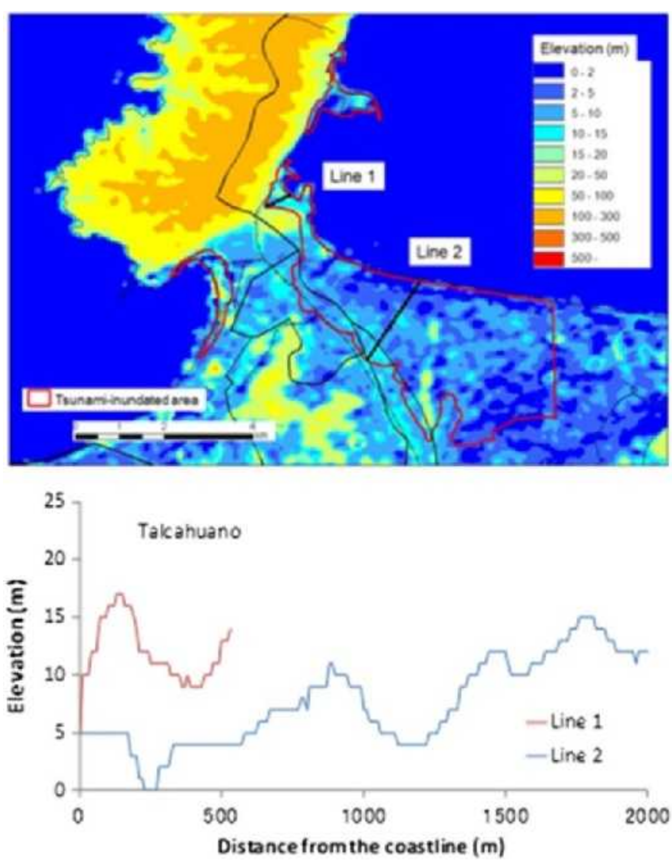

Figure 6. Tsunami-inundated areas and distribution of the elevations in Talcahuano and elevations along the transverse lines.

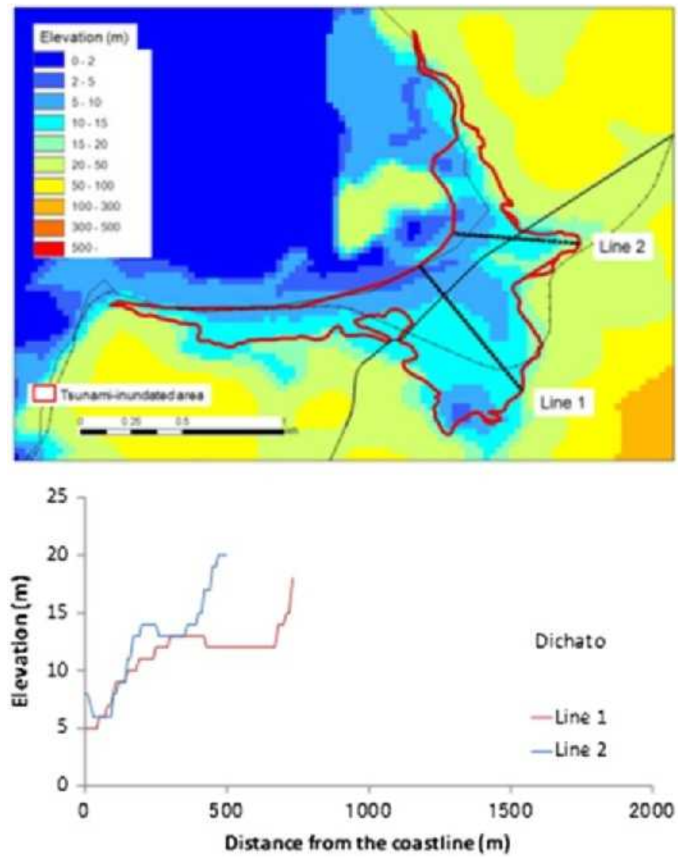

Figure 7. Tsunami-inundated areas and distribution of the elevations in Dichato and elevations along the transverse lines.

elevations are presented with respect to their distance from the Maule River. The relatively low elevations and slow grades result in long travel distances of the tsunami wave. According to Line 2 in Talcahuano, the tsunami wave could travel approximately 2,000 m from the coastline.

Line 1 in Constitución was assigned to identify the surveyed site by Imamura et al. (2010). According to their report, the tsunami runup height was 28.3 m at the site. Since the DEM used in this study is a global dataset that consists of 30 m grid cells, the elevation at the site is estimated to be approximately 23 m. The slope is estimated to be approximately 67% and is almost equivalent to that reported by Imamura et al. (2010), 63.5%. Since ASTER GDEM covers all the land on the earth homogeneously with the resolution of 30 m, this spatial information can be applicable for various areas where the GIS dataset is not well developed to draw damage estimation and disaster mitigation plan due to earthquakes and tsunamis.

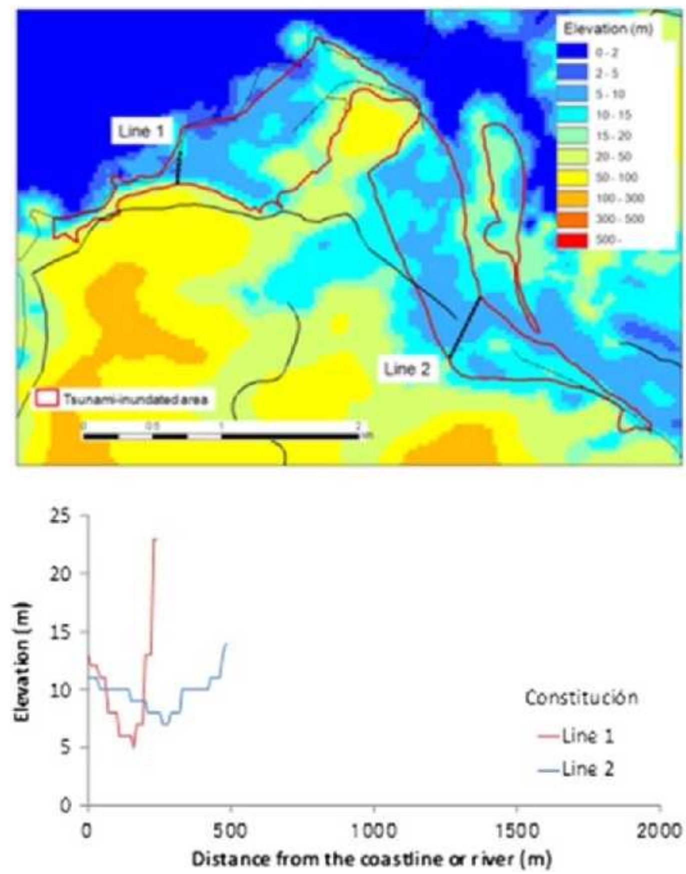

Figure 8. Tsunami-inundated areas and distribution of the elevations in Constitución and elevations along the transverse lines.

CONCLUSIONS

In this paper, the results of a field survey conducted after the 2010 Chile earthquake by the authors during 2–8 April 2010 are presented. The availability of satellite images to detect damage to buildings is discussed, employing the field photos taken in Concepción. The GIS dataset for the building damage in Talca was developed by establishing the location of the image file in terms of map projections. The usefulness of high-resolution satellite images to detect the building damage in Talca was also investigated with the aid of the constructed GIS dataset. Moreover, the tsunami inundation maps published by ONEMI were georeferenced, and the characteristics of the inundated areas were evaluated in view of the elevation.

According to the comparisons between satellite images and field photos in Concepción, various affected structures could be visually detected. However, it seemed that damaged unreinforced masonry buildings were difficult to be identified in the satellite image in Concepción. The similar tendency was also found in the satellite image which captured damaged buildings in Talca, which were mainly adobe and unreinforced masonry buildings. Some of the affected buildings could be visually detected, but not all the damaged ones could be identified appropriately. Since the post-event satellite image was captured with a large off-nadir angle, the quality of the image was not fine enough to detect damage to relatively small buildings.

According to the relationship between the building damage levels and the lot areas in Talca, the mean of the areas associated with the nondamaged buildings was the smallest, while the mean of the areas associated with the buildings to be removed was the largest. In Talca, modern buildings that were designed according to the current codes suffered minor, repairable damage, while a large number of adobe and unreinforced masonry constructions, which were built in the 1960s–70s, suffered significant damage. On the basis of these circumstances, it has been speculated that the newer buildings may be constructed in relatively small lots; however, the construction periods are not available at this moment.

A comparison of the georeferenced tsunami-inundated areas with the elevations obtained from the ASTER GDEM revealed that the elevations in the inundated areas were lower than 20 m on the whole except for a certain area. The steepest slope is estimated to be approximately 67% and is almost equivalent to that reported by the field survey of the other research group. Although the accuracy is limited, ASTER GDEM works for disaster mitigation planning in the areas where the GIS dataset is not well developed.

These findings of our field survey after the 2010 Chile earthquake will be expanded in the earthquake and tsunami disaster mitigation technology in Peru through the SATREPS project.

ACKNOWLEDGMENTS

The authors would like to express their sincere gratitude to the Japan Science and Technology Agency (JST) for the financial support in conducting the field survey under the SATREPS project "Enhancement of earthquake and tsunami disaster mitigation technology in Peru" (Principal Investigator: F. Yamazaki, Chiba University).

REFERENCES

Boroschek, R., Soto, P., and Leon, R., 2010. *Maule Region Earthquake 27 February 2010* M_w *= 8.8*, http://www.eqclearinghouse.org/20100227-chile/maps/report-on-strong-motion-records-from-univ-of-chile.

Bray, J., and Frost, D., 2010. *Geo-Engineering Reconnaissance of the 2010 Maule, Chile Earthquake*, Geotechnical Extreme Events Reconnaissance (GEER) Association, http://www.geerassociation.org/GEER_Post%20EQ%20Reports/Maule_Chile_2010/Maule_Chile_2010_index.html.

Campbell, J. B., 2006. *Introduction to Remote Sensing*, Fourth Edition, The Guilford Press, New York, 626 pp.

Chen, P., Liew, S. C., and Kwoh, L. K., 2005. Tsunami damage assessment using high resolution satellite imagery: A case study of Aceh, Indonesia, in *Proceedings of the International Geosciences and Remote Sensing Symposium, IGARSS 2005*, 1405–1408.

Earth Remote Sensing Data Analysis Center (ERSDAC), 2009. *Advanced Spaceborne Thermal Emission and Reflection Global Digital Elevation Map (ASTER GDEM)*, http://www.gdem.aster.ersdac.or.jp/.

Earthquake Engineering Research Institute (EERI), 2010a. *Report from Structural Team 3/17/10*, Oakland, CA, http://www.eqclearinghouse.org/20100227-chile/reports-from-the-field/report-from-structural-team-31710.

Earthquake Engineering Research Institute (EERI), 2010b. *Report from the Bridge Team*, 3/18, Oakland, CA, http://www.eqclearinghouse.org/20100227-chile/reports-from-the-field/report-from-the-bridge-team-318.

Earthquake Engineering Research Institute (EERI), 2010c. *Report from Social Science and Policy Team–Talca and Constitución*, Oakland, CA, http://www.eqclearinghouse.org/20100227-chile/reports-from-the-field/report-from-guillermo-franco-talca-and-constitucion.

Eguchi, R. T., Huyck, C. K., Ghosh, S., and Adams, B. J., 2008. The application of remote sensing technologies for disaster management, in *Proceedings of The 14th World Conference on Earthquake Engineering*, Paper ID. K004, 17 pp.

Imamura, F., Fujima, K., and Arikawa, T., 2010. *Field Survey of the 2010 Chilean Tsunami*, Japan Society of Civil Engineers, http://www.jsce.or.jp/committee/eec2/eq_report/201003Chile/Imamura.pdf.

Japan Science and Technology Agency (JST), 2008. *Science and Technology Research Partnership for Sustainable Development*, http://www.jst.go.jp/global/english/index.html.

Jet Propulsion Laboratory, 2009. *Shuttle Radar Topography Mission (SRTM)*, http://www2.jpl.nasa.gov/srtm/index.html.

Kouchi, K., and Yamazaki, F., 2007. Characteristics of tsunami-affected areas in moderate-resolution satellite images, in *Transactions on Geoscience and Remote Sensing*, IEEE, **45**, 1650–1657.

MCEER, 2010. *Preliminary Damage Reports from the Chile Earthquake: 27 February 2010*, University at Buffalo, State University of New York, http://mceer.buffalo.edu/research/Reconnaissance/Chile2-27-10/damage-reports.asp.

Miura, H., Wijeyewickrema, A. C., and Inoue, S., 2006. Evaluation of tsunami damage in the eastern part of Sri Lanka due to the 2004 Sumatra earthquake using remote sensing technique, in *Proceedings of 100th Anniversary 1906 San Francisco Earthquake Conference*, Paper No. 8NCEE-856.

Rathje, E. M., and Adams, B. J., 2008. The Role of Remote Sensing in Earthquake Science and Engineering: Opportunities and Challenges, *Earthquake Spectra* **24**, 471–492.

ReliefWeb, 2010. *Chile: Earthquake – February 2010*, http://www.reliefweb.int/rw/dbc.nsf/doc108? OpenForm&emid=EQ-2010-000034-CHL&rc=2.

Ruegg, J. C., Rudloff, A., Vigny, C., de Chabalier, J. B., Campos, J., Kausel, E., Barrientos, S., and Dimitrov, D., 2009. Interseismic strain accumulation measured by GPS in the seismic gap between Concepción–Constitución in Chile, *Physics of Earth and Planetary Interiors* **175**, 78–85.

Saito, K., Spence, R., Going, C., and Markus, M., 2004. Using high-resolution satellite images for post-earthquake building damage Assessment: A study following the 26 January 2001 Gujarat earthquake, *Earthquake Spectra* **20**, 145–169.

The National System of Coordination of Territorial Information (SNIT), 2010. *Terremoto 2010*, http://www.snit.cl/terremoto2010/.

U.S. Geological Survey (USGS), 2010. *ShakeMap us2010tfan*, http://earthquake.usgs.gov/earthquakes/shakemap/global/shake/2010tfan/.

Yamazaki, F., Yano, Y., and Matsuoka, M., 2005. Visual damage interpretation of buildings in Bam City using QuickBird images following the 2003 Bam, Iran, earthquake, *Earthquake Spectra* **21**, S1, 329–336.

Yamazaki, F., Zavala, C., Nakai, S., Koshimura, S., Saito, T., and Midorikawa, S., 2010. Enhancement of earthquake and tsunami Disaster mitigation technology in Peru: A SATREPS project, in *Proceedings of the 7th International Conference on Urban Earthquake Engineering*, Tokyo, Japan, 1501–1506.

(Received 3 January 2011; accepted 6 February 2012)